Journal of Applied Polymer Science

Thermal Degradation Behavior and Gas Phase Flame-Retardant Mechanism of Polylactide/PCPP Blends

Haijuan Lin,[1,2] Lijing Han,[1] Lisong Dong[1]

[1]Key Laboratory of Polymer Ecomaterials (KLPE), Changchun Institute of Applied Chemistry, Chinese Academy of Sciences, Changchun 130022, People's Republic of China

[2]University of Chinese Academy of Sciences, Beijing 100049, People's Republic of China

Correspondence to: L. Dong (E-mail: dongls@ciac.ac.cn)

ABSTRACT: The thermal degradation behavior of the blend based on polylactide (PLA) and poly(1,2-propanediol 2-carboxyethyl phenyl phosphinate) (PCPP) was investigated by the thermogravimetric analysis (TGA). Thermal degradation activation energies (E_a) of neat PLA and PLA/15% PCPP blend were calculated via the Flynn–Wall–Ozawa method. The E_a of the blends increased with the addition of PCPP increasing when the conversion was higher than 10%. In addition, the appropriate conversion models for the thermal degradation process of PLA and PLA/15% PCPP were studied via the Criado method. At the same time, the main gaseous decomposition products of PLA and its blend were identified by TGA/infrared spectrometry (TGA–FTIR) analysis. And it revealed that the PCPP improved the flame-retardant property of PLA via altering the release of the flammable gas and nonflammable gas. Moreover, the PCPP improved the flame-retardant property of PLA by inhibiting exothermic oxidation reactions in the combustion, which was further proved by pyrolysis–gas chromatography–mass spectrometry analysis. © 2014 Wiley Periodicals, Inc. J. Appl. Polym. Sci. **2014**, *131*, 40480.

KEYWORDS: thermogravimetric analysis (TGA); polylactide; blends; flame retardance

Received 22 October 2013; accepted 19 January 2014

DOI: 10.1002/app.40480

INTRODUCTION

Recently, polymers derived from renewable resources have been achieved much attention with the elevated environmental awareness of the public. Polylactide (PLA) is a kind of aliphatic polyester made up of lactic acid (2-hydroxy propionic acid) as building blocks and also a biodegradable thermoplastic derived from renewable sources such as starch and sugar. Because of its biodegradability and relatively good mechanical strength, PLA has been considered as one of the most important bio-based polymers. In the last decade, the main uses of PLA have been limited to medical applications such as implant devices, tissue scaffolds, and internal sutures. In recent years, PLA has been used as an ideal material for food packaging due to its environmentally benign characteristics.[1–4] Now the expected market of PLA should be rapidly extended to transportation, electrical and electronic equipment sectors. However, its flammability strongly limits its further use in the applications in which nonflammable material is required. So it is clear that the improving of the flame-retardant property of PLA is becoming an issue in recent years.

Now, more and more patents and technical works are interested in the halogen-free solutions because the halogenated compounds will produce poisonous and corrosive smoke, and release the toxic hydrogen halide.[5] The predominance of the studies on halogen-free flame retardants focuses on phosphorus-based products. In recent years, more different phosphorus-containing flame retardants for the plastics are investigated. And they were proved as particularly effective flame retardants in polymer containing oxygen such as polyesters, polyamides, cellulose, etc.[6,7] In addition, the flame-retardant mechanism of phosphorus-containing flame retardant has been reported as follows. In the condensed phase, the thermal decomposition of phosphorus-containing flame retardants is ready to produce pyrophosphate structures and liberate water. The water released dilutes the oxidizing gas phase. And the phosphoric acid and pyrophosphoric acid can catalyze the dehydration reaction. Phosphorus-containing flame retardants can also volatilize into the gas phase to form active radicals ($PO_2\cdot$, $PO\cdot$, and $HPO\cdot$) which act as scavengers of $H\cdot$ and $OH\cdot$ radicals.[8]

In our previous study,[9] we had synthesized the flame retardant PCPP and prepared PLA/PCPP blend by direct melt compounding successfully. And the PCPP was confirmed as an effective flame retardant for the PLA as evidenced by increasing limiting oxygen index (LOI) value. The LOI value increased from 19.7

Table I. Algebraic Expressions of Functions of the Most Common Reaction Mechanisms

Mechanism	f(x)	g(x)
Power law (P2)	$2x^{1/2}$	$x^{1/2}$
Power law (P3)	$3x^{2/3}$	$x^{1/3}$
Power law (P4)	$4x^{3/4}$	$x^{1/4}$
Avarami-Erofe'ev(A2)	$2(1-x)[-\ln(1-x)]^{1/2}$	$[-\ln(1-x)]^{1/2}$
Avarami-Erofe'ev(A3)	$3(1-x)[-\ln(1-x)]^{2/3}$	$[-\ln(1-x)]^{1/3}$
Avarami-Erofe'ev(A4)	$4(1-x)[-\ln(1-x)]^{3/4}$	$[-\ln(1-x)]^{1/4}$
Contracting Sphere (R2)	$2(1-x)^{1/2}$	$[1-(1-x)^{1/2}]$
Contracting Sphere (R3)	$3(1-x)^{2/3}$	$[1-(1-x)^{1/3}]$
One-dimensional diffusion(D1)	$1/2x$	x^2
One-dimensional diffusion(D2)	$[-\ln(1-x)]^{-1}$	$[(1-x)\ln(1-x)]+x$
One-dimensional diffusion, Jander(D3)	$3(1-x)^{2/3}/[2(1-(1-x)^{1/3})]$	$[(1-(1-x)^{1/3})]^2$
Ginstling-Brounshtein (D4)	$3/2((1-x)^{-1/3}-1)$	$1-(2x/3)-(1-x)^{2/3}$
First-order (F1)	$(1-x)$	$-\ln(1-x)$
Second-order (F2)	$(1-x)^2$	$(1-x)^{-1}-1$
Third-order (F3)	$(1-x)^3$	$[(1-x)^{-2}-1]/2$

O_2% for the neat PLA to 28.2 O_2% for the PLA/10% PCPP blend. PLA blends showed UL-94 V-0 rating only by the addition of low amounts of 3 wt % PCPP. Additionally, the flame-retardant and the mechanical properties were improved simultaneously when the content of PCPP in the blends was up to 15 wt %. As a further investigation, in this study, we reported the thermal degradation behaviors of PLA and its blend in order to investigate the thermal degradation process in detail. In addition, the action of PCPP in the gas phase to improve the flame-retardant property of PLA was studied as well.

EXPERIMENTAL

Materials

PLA resin (4032D) from Natureworks with a weight-average molecular weight of 207 kDa and polydispersity of 1.73 (GPC analysis) was used in this study. Poly(1,2-propanediol 2-carboxyethyl phenyl phosphinate) (PCPP) was synthesized with 2-carboxyethyl phenylphosphinic acid (CEPPA) and 1,2-propanediol (PD) in our laboratory.[9]

Preparation of PLA Blends

PLA was dried in a vacuum oven at 80°C for 12 h. The samples were prepared by using a Haake batch intensive mixer (Haake Rheomix 600, Karlsruhe, Germany) at the temperature of 180°C with the roller speed of 60 rpm for 10 min. The ratio of PCPP to PLA in the PLA/15% PCPP blend is 15 : 100 (wt/wt). After mixing, samples were hot-pressed under 5 MPa for 3 min at 190°C followed by cold-press at room temperature to form sheets for all tests.

Measurements

PLA and PLA/15% PCPP were subjected to the thermogravimetric analysis (TGA; Perkin-Elmer TGA-7) in a nitrogen atmosphere at different heating rates (5°C/min, 10°C/min,

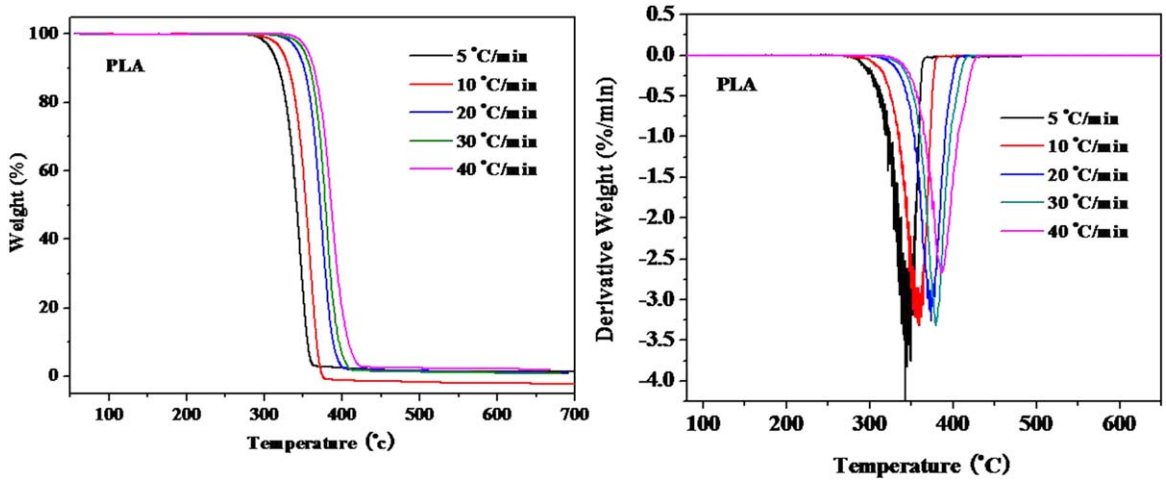

Figure 1. The TGA and derivative thermogravimetric curves of PLA at the different heating rates. [Color figure can be viewed in the online issue, which is available at wileyonlinelibrary.com.]

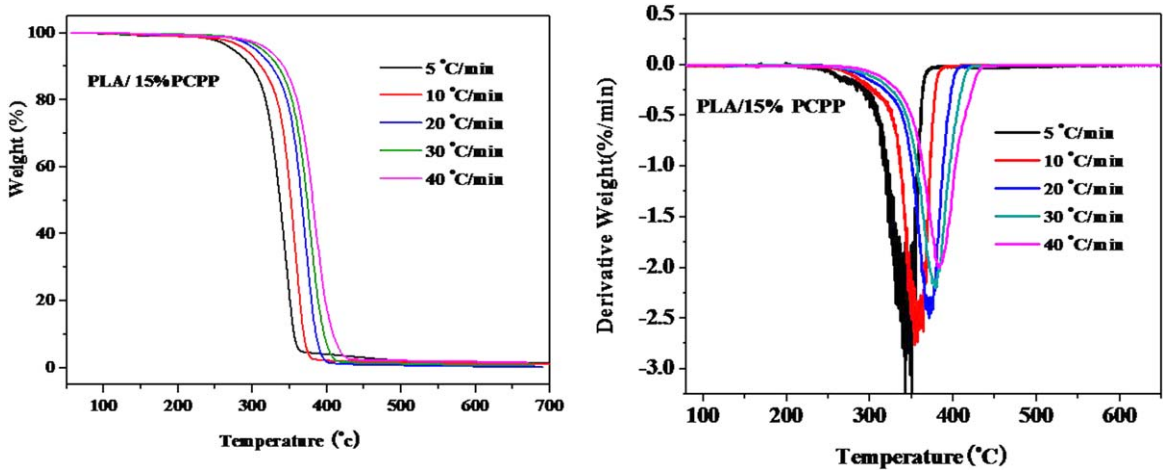

Figure 2. The TGA and derivative thermogravimetric curves of PLA/15% PCPP at the different heating rates. [Color figure can be viewed in the online issue, which is available at wileyonlinelibrary.com.]

20°C/min, 30°C/min, and 40°C/min) from room temperature to 700°C.

TGA/infrared spectrometry (TGA-FTIR) analysis of PLA and PLA/15% PCPP was performed via the TGA-7 thermogravimetric analyzer interfaced to a Nicolet 6700 FTIR spectrometer. About 10.0 mg of sample was put in an alumina crucible and heated from 25°C to 700°C at nitrogen atmosphere (flow rate of 60 mL/min). The heating rate was 10°C /min.

Pyrolysis–gas chromatography–mass spectrometry (Py–GC–MS) analysis was carried out on a GC–MS (Agilent 5975–6890N). This experiment was performed using the standard direct insertion probe for solid polymer materials. The oven temperature was programmed as follows: from room temperature to 350°C or 450°C at the heating rate of 20°C/min, and held at 350°C or 450°C for 3 min. This experiment was performed under inert (helium) atmosphere.

Theoretical Consideration

Dynamic TGA method is a great promise tool to investigate the mechanism of physical and chemical processes that occur during the polymer degradation. All kinetic studies assume that the isothermal rate of conversion $d\alpha/dt$, is a linear function of a temperature-dependent rate constant, k, and a temperature-independent function of the conversion α, that is:

$$\frac{d\alpha}{dt} = kf(\alpha) \tag{1}$$

where $f(\alpha)$ and k are functions of conversion and temperature, respectively.

According to Arrhenius,

$$k = Ae^{-\frac{E_\alpha}{RT}} \tag{2}$$

where E_α is the activation energy, A is the pre-exponential factor, and R is the gas constant.

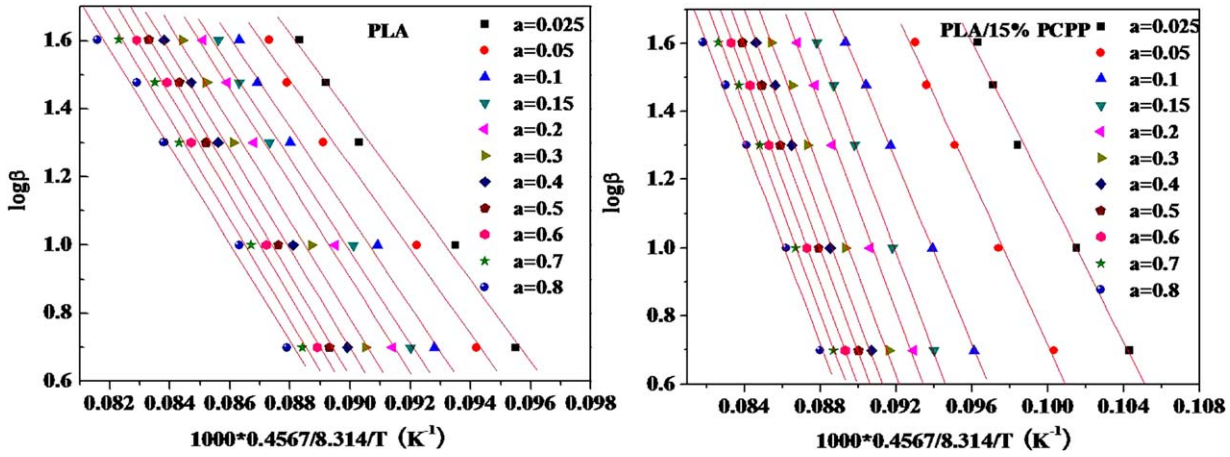

Figure 3. FWO plots at the following different weight loss of PLA and PLA/15% PCPP blend. [Color figure can be viewed in the online issue, which is available at wileyonlinelibrary.com.]

Table II. Activation Energies of PLA and PLA/15% PCPP Obtained by FWO Method

	PLA		PLA/15% PCPP	
Conversion α	*E* (kJ/mol)	*r*	*E* (kJ/mol)	*r*
0.025	120.4 (±0.03)	0.9961	110.1 (±0.06)	0.9976
0.05	123.6 (±0.04)	0.9953	122.1 (±0.05)	0.9971
0.10	131.8 (±0.05)	0.9955	134.0 (±0.01)	0.9997
0.15	135.3 (±0.02)	0.9963	146.9 (±0.03)	0.997
0.20	138.9 (±0.03)	0.9968	149.7 (±0.01)	0.9982
0.30	143.7 (±0.05)	0.9971	148.9 (±0.03)	0.9975
0.40	145.2 (±0.02)	0.9979	150.4 (±0.01)	0.9987
0.50	148.7 (±0.01)	0.9979	150.1 (±0.04)	0.9995
0.60	148.1 (±0.03)	0.9971	152.3 (±0.01)	0.9996
0.70	147.9 (±0.02)	0.9969	150.9 (±0.03)	0.9991
0.80	142.6 (±0.03)	0.9955	147.2 (±0.04)	0.9981

The $f(\alpha)$ depends on the particular decomposition mechanism. The simplest and most frequently used model for $f(\alpha)$ in the analysis of TGA data is

$$f(\alpha) = (1 - \alpha)^n \tag{3}$$

where n is the order of reaction, insertion of eqs. (2) and (3) into eq. (1) gives

$$\frac{d\alpha}{dt} = \beta \frac{d\alpha}{dT} = A(1-\alpha)^n e^{-\frac{E_\alpha}{RT}} \tag{4}$$

Flynn–Wall–Ozawa Method (FWO)[10]

FWO method is one of integral methods that can determine the activation energy without knowledge of reaction order. It is used to determine the activation energy directly from weight loss versus temperature data obtained at several heating rates. Equation (4) is integrated using Doyle's approximation[11] and then the integration after taking logarithms is:

$$\log F(a) = \log \frac{AE_\alpha}{R} - \log \beta - 2.315 - 0.4567 \frac{E_\alpha}{RT} \tag{5}$$

where A and E_a have the same meanings as above, β is the heating rate, and $F(a)$ is the integral function of conversion. Activation energies for different conversion values can be calculated from log β versus $1/T$ plot. And the activation energy is denoted as apparent activation energy throughout this study since the activation energy derived from TGA data is the sum of activation energies of chemical reaction and physical process.[12]

Criado Method[13,14]

The kinetic model of the process can be determined by the Criado method. The equation is shown as:

$$\frac{Z(x)}{Z(0.5)} = \frac{f(x)g(x)}{f(0.5)g(0.5)} = \left(\frac{T_x}{T_{0.5}}\right)^2 \frac{(dx/dt)_x}{(dx/dt)_{0.5}} \tag{6}$$

where 0.5 refers to the conversion in $x = 0.5$. The left side of eq. (6) $\frac{f(x)g(x)}{f(0.5)g(0.5)}$ is a reduced theoretical curve, which corresponds to each reaction mechanism shown in Table I, but the right side of the equation associated with the fixed heating rate can be obtained from experimental data. A comparison of both sides of eq. (6) tells us which kinetic model describes an experimental reactive process. Table I indicates the algebraic expressions of $f(x)$ and $g(x)$ for the kinetic models used. And the heating rate in this analysis is 10°C/min.

RESULTS AND DISCUSSION

Thermal Degradation

Figures 1 and 2 show the TGA and DTG curves for PLA and PLA/15% PCPP blend at different heating rates (5°C/min, 10°C/min, 20°C/min, 30°C/min, and 40°C/min), respectively. It can be seen from Figures 1 and 2 that PLA begins to decompose at 338°C and the temperature of maximum decomposition (T_{max}) is about 359°C when the heating rate is 10°C/min. Meanwhile, the temperature of the beginning degradation for PLA/15% PCPP blend is 331°C and T_{max} is 355°C with the same heating rate of 10°C/min. The temperature of the beginning degradation for PLA/15% PCPP blend is lower than that of PLA, which is attributed to the relatively low decomposition temperature of PCPP. In addition, with increasing the heating rate, the TGA curve shifts to higher temperature. This result is consistent with the fact that the degradation is a function of

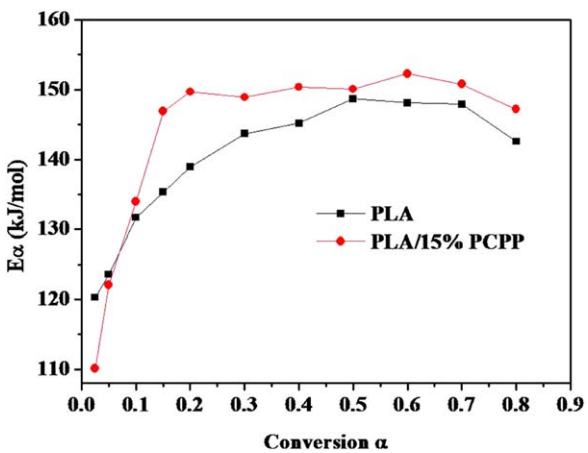

Figure 4. The plots of activation energy (E_α) versus conversion (α). [Color figure can be viewed in the online issue, which is available at wileyonlinelibrary.com.]

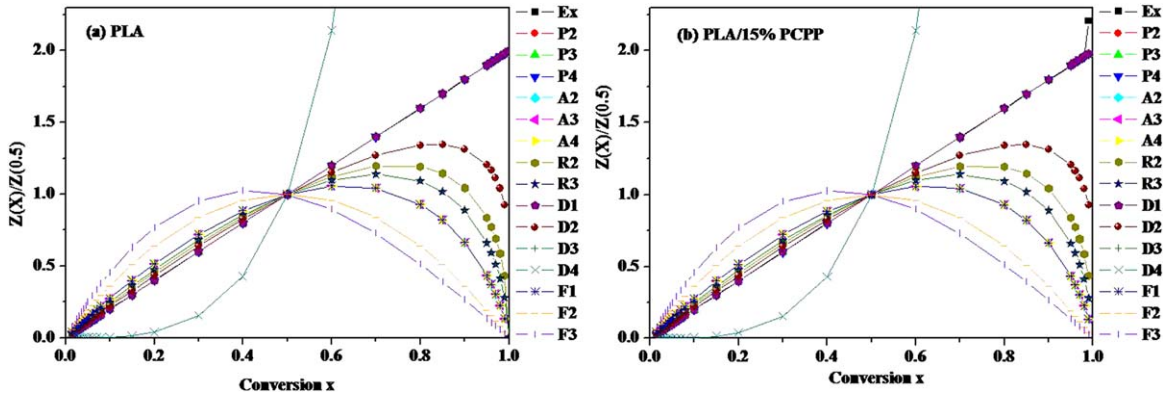

Figure 5. Masterplots of different kinetic models and experiment data at 10°C/min calculated by Criado method for (**a**) PLA and (**b**) PLA/15% PCPP. [Color figure can be viewed in the online issue, which is available at wileyonlinelibrary.com.]

both temperature and time. As DTG curves shown, at a constant heating rate, the first derivative of TGA weight loss curve of PLA has a single peak, which implies that there is only a single stage during the thermal degradation of PLA.[15,16] However, the DTG curves of PLA/15% PCPP show two stages degradation behavior, particularly at the 5°C/min heating rate. The first stage is belonging to the degradation of PCPP, and the second stage would be due to the thermal degradation of PLA.

Calculation of the Activation Energy

The FWO method is a well-known representative of model-free approach. And this method is used to evaluate the thermal degradation behavior of PLA and PLA/15% PCPP blend here. As shown in Figure 3, the fitting lines are straight lines with a good correlation coefficient *r*, which indicates FWO method is applicable to the systems in the conversion range investigated. The activation energies of PLA and PLA/15% PCPP blend for

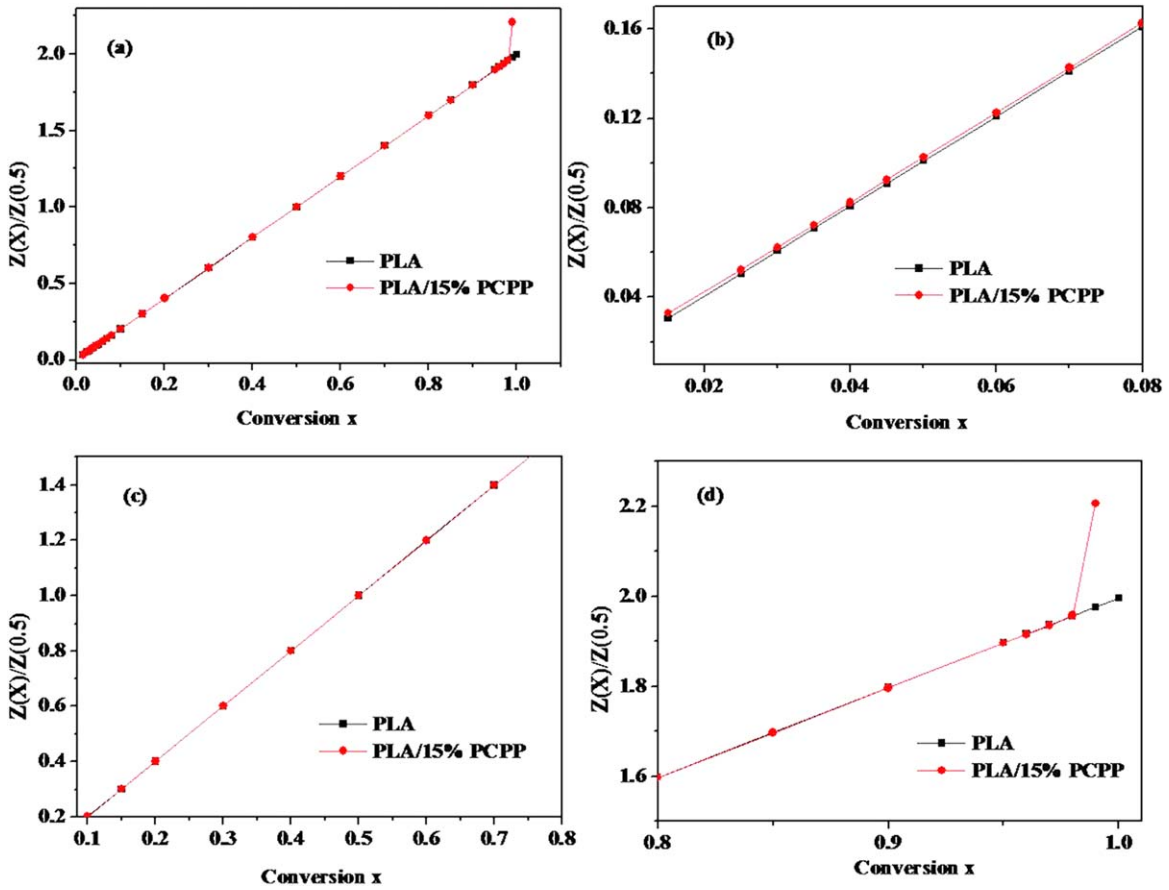

Figure 6. Plots of experiment data calculated by Criado method for PLA and PLA/15% PCPP (**a**) conversion from 0% to 100%; (**b**) conversion from 0% to 8%; (**c**) conversion from 10 to% 80%; and (**d**) conversion from 80% to 100%. [Color figure can be viewed in the online issue, which is available at wileyonlinelibrary.com.]

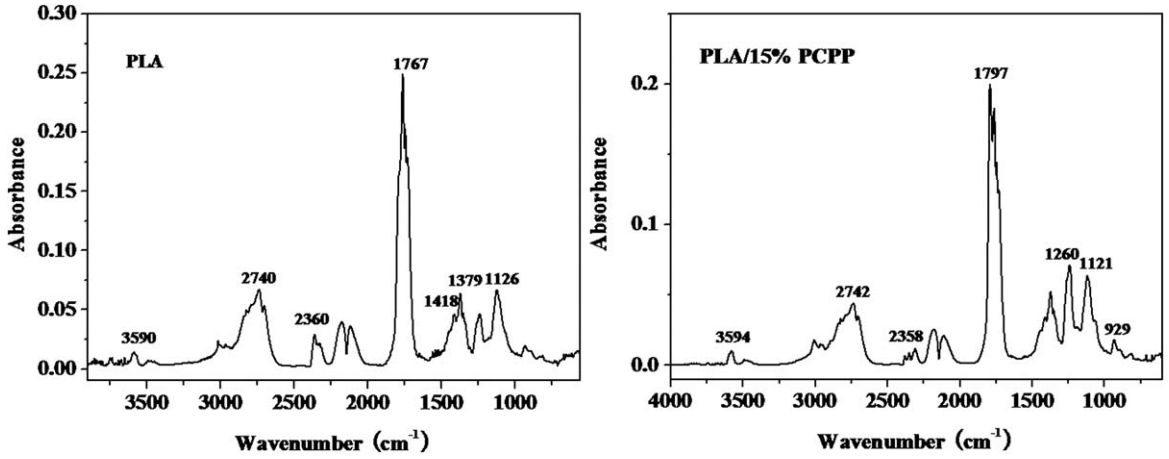

Figure 7. FTIR spectra of pyrolysis products for PLA and PLA/15% PCPP at the maximum decomposition rate.

different conversions are revealed in Table II. The plots of activation energy (E_α) versus conversion (α) were shown in Figure 4. As it can be seen, the apparent E_a of PLA steadily increases from 120 to 145 kJ/mol with an increase in conversion at the initial thermal degradation. And it almost has a plateau with the E_a converges at about 148 kJ/mol in the range of 50%–70% conversion. However, the initial apparent activation energy of PLA blend with the addition of 15 wt % PCPP is found to be about 10 kJ/mol lower than that of PLA. The apparent E_a of PLA/15% PCPP blend is higher than that of PLA at the same conversion, but shows the same changing trend as that revealed in the PLA as the conversion ranges from 10% to 100%.

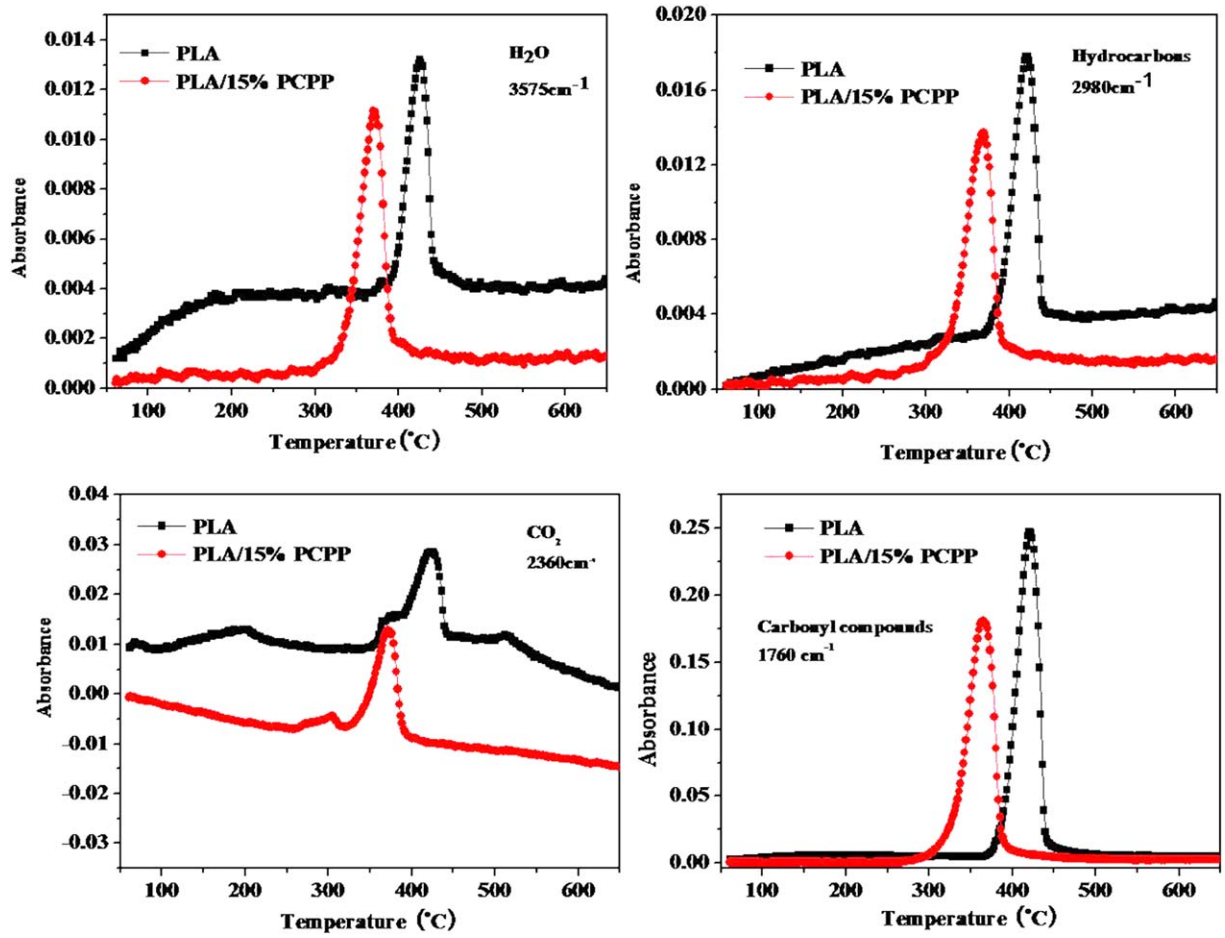

Figure 8. Absorbance of pyrolysis products for PLA and PLA/15% PCPP versus temperature. [Color figure can be viewed in the online issue, which is available at wileyonlinelibrary.com.]

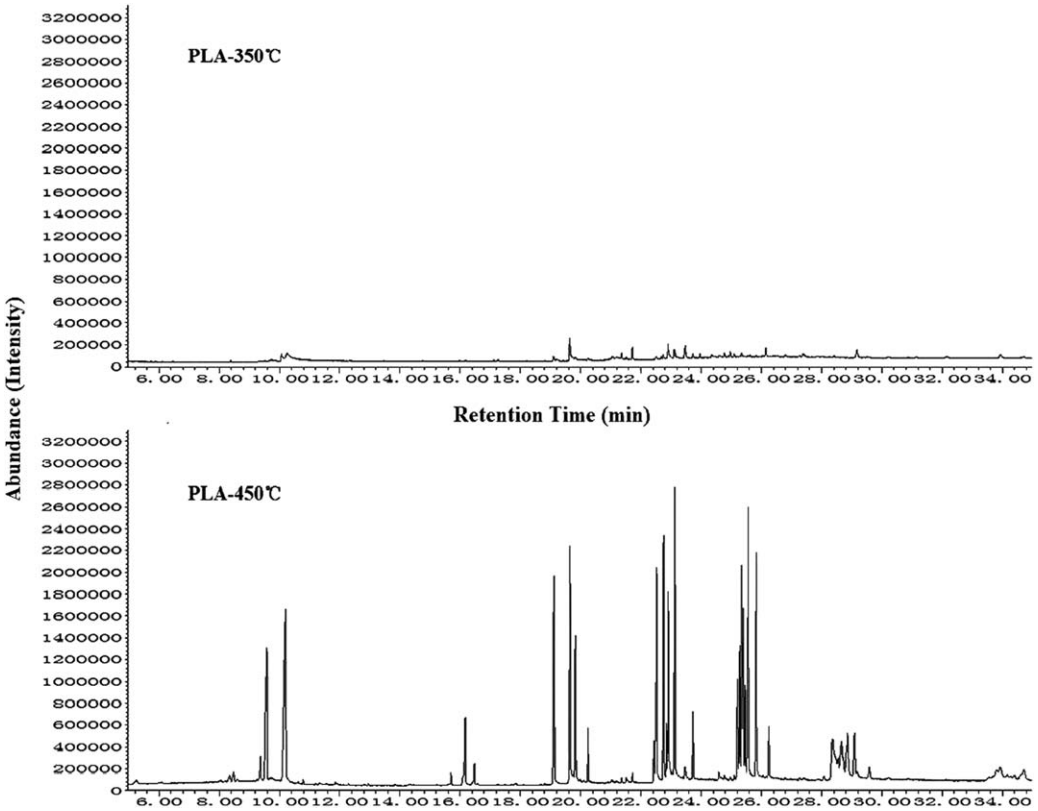

Figure 9. Py–GC–MS chromatograms of pyrolyzates from PLA.

Evidently, the E_a at the initial stage of the degradation (before 5% conversion) decreases with the addition of the PCPP due to the lower stability of P—O—C bond in PCPP compared with the C—C bond. And the degraded phosphate group could assist in the formation of thermally stable compounds, which could slow down further degradation of PLA. And so the apparent E_a values of PLA blend increase.

Determination of the Degradation Mechanism Using Criado Method

The $Z(x)/Z(0.5)$ master curves can be plotted using eq. (6) according to different reaction mechanisms $g(x)$ shown in Table I. In this section, the used experimental TGA data are from TGA curve at the heating rate of 10°C/min. The $Z(x)/Z(0.5)$ master and experimental curves of PLA and PLA/15% PCPP are

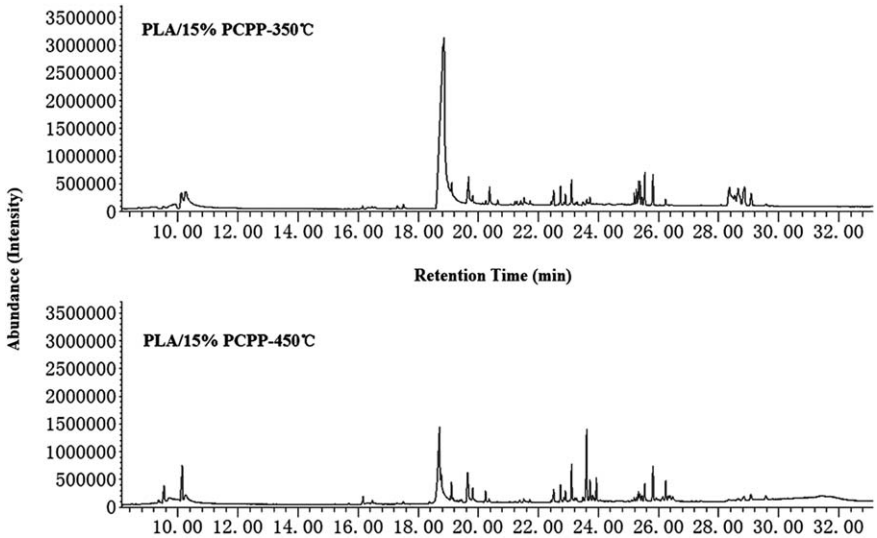

Figure 10. Py–GC–MS chromatograms of pyrolyzates from PLA/15% PCPP.

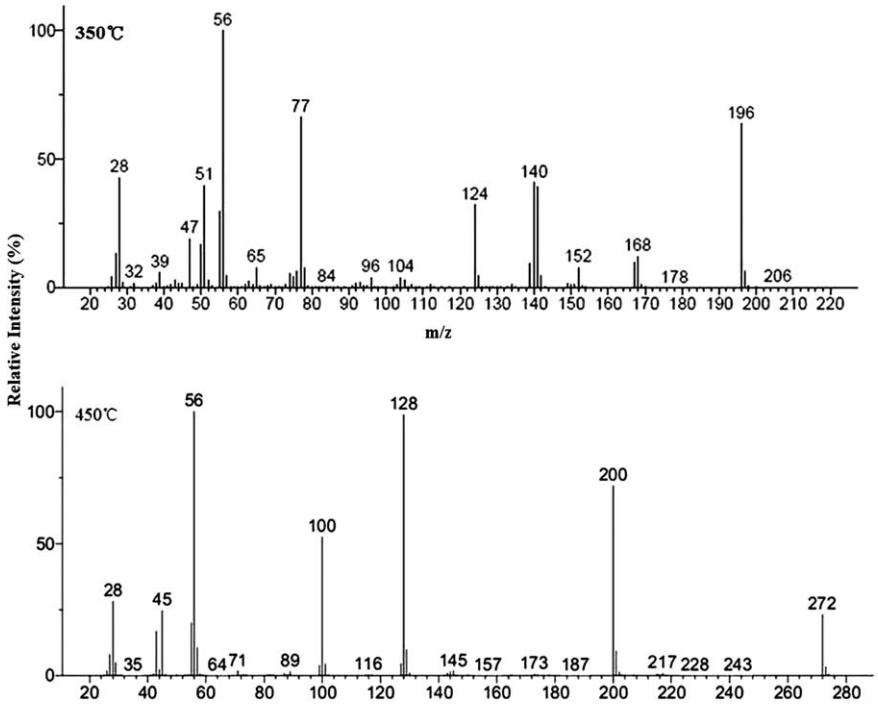

Figure 11. MS spectra of compounds evolved from PLA/15% PCPP blends at different temperatures.

shown in Figure 5(a,b), respectively. We could find that the experimental curve of PLA nearly overlaps the master curve $Z(x)/Z(0.5)$ belonging to P3 (power law) reaction mechanism. However, the experimental curve of PLA/15% PCPP deviates slightly from the master curve of P3 reaction mechanism before 5 % conversion [Figure 6(b)]. And at the range of 10%–90% conversion, the experimental curve of PLA/15% PCPP accord with the curve of PLA [Figure 6(c)]. After 90% conversion, the experimental curve of blend deviates from the master curve again [Figure 6(d)]. In conclusion, for PLA/15% PCPP blend, the PCPP decomposes firstly inducing a slight change of the kinetic model; with the temperature increasing, PLA decomposes, so the main kinetic mechanism of the blend is the same as that of PLA. After 90% conversion, the products from the degradation of PCPP react with the products from the degradation of PLA to become thermally stable compounds, so the kinetic mechanism of the degradation process of blend is different from that of neat PLA.

TGA–FTIR Analysis of PLA and PLA/15% PCPP Blend

TGA–FTIR was used to investigate the gaseous products released during the thermal degradation of PLA and PLA/PCPP blend. As shown in Figure 7, the gaseous products of PLA at maximum decomposition rate include characteristic bands of H_2O (3575 cm^{-1}), CO_2 (2360 cm^{-1}), hydrocarbons (—CH_3 and —CH_2— groups, 2980–2850 cm^{-1} and 1200–1400 cm^{-1}), compounds containing carbonyl group (1760 cm^{-1}), etc.[17–19] And the main gaseous products for PLA/15% PCPP at the maximum decomposition rate are similar to that of PLA. Moreover, new absorption bands at 1260 cm^{-1}(P═O) and 1121 cm^{-1}(—P—O—P—O) indicate that the polyphosphate structures are formed by decomposition of PCPP.[20,21] The absorbance of pyrolysis products for PLA and PLA/15% PCPP versus temperature is revealed in Figure 8. PLA begins to release pyrolysis products at about 350°C, while PLA/15% PCPP begins to release pyrolysis products at about 300°C, which is earlier than pure PLA. This is likely due to the low decomposition temperature of PCPP. As shown in the Figure 8, the absorbance intensity of pyrolysis products for the PLA/15% PCPP is lower than that of neat PLA. In other words, PCPP reduces the release of gaseous products and the weight loss. Especially, the decrease of flammable gas release (such as hydrocarbons) could reduce the combustion time, which is in favor of improving the flame-retardant property of PLA. We can come to the conclusion that in the presence of phosphorus, the main composition of the pyrolysis gases remains unchanged. So the flame-retardant activity seems to be connected with a shift in the release of flammable and nonflammable pyrolysis products rather than with a basic change of the pyrolysis pattern. This result accords with the analysis of the thermal degradation via Criado method.

Py–GC–MS Analysis of PLA and PLA Blend

Pyrolysis products of PLA and PLA/15% PCPP blend at the temperature of 350°C and 450°C were analyzed by Py–GC–MS. The results are shown in the Figures 9 and 10. For the neat PLA, the small amount of pyrolysis products is detected at the temperature of 350°C. When the temperature increases to 450°C, the lactides [11.8 min (meso-lactide)] and cyclic oligomers in the range of 20–30 min are detected.[22] As reported previously, the pyrolysis of neat PLA results in the production of a large amount of cyclic oligomers through the random degradation process.[23] So it can be concluded that PLA pyrolyses mainly at the temperature of 450°C here. For the PLA/15% PCPP blend, the phosphorus-containing compound (18.6 min) is detected at the temperature of 350°C. However, when the

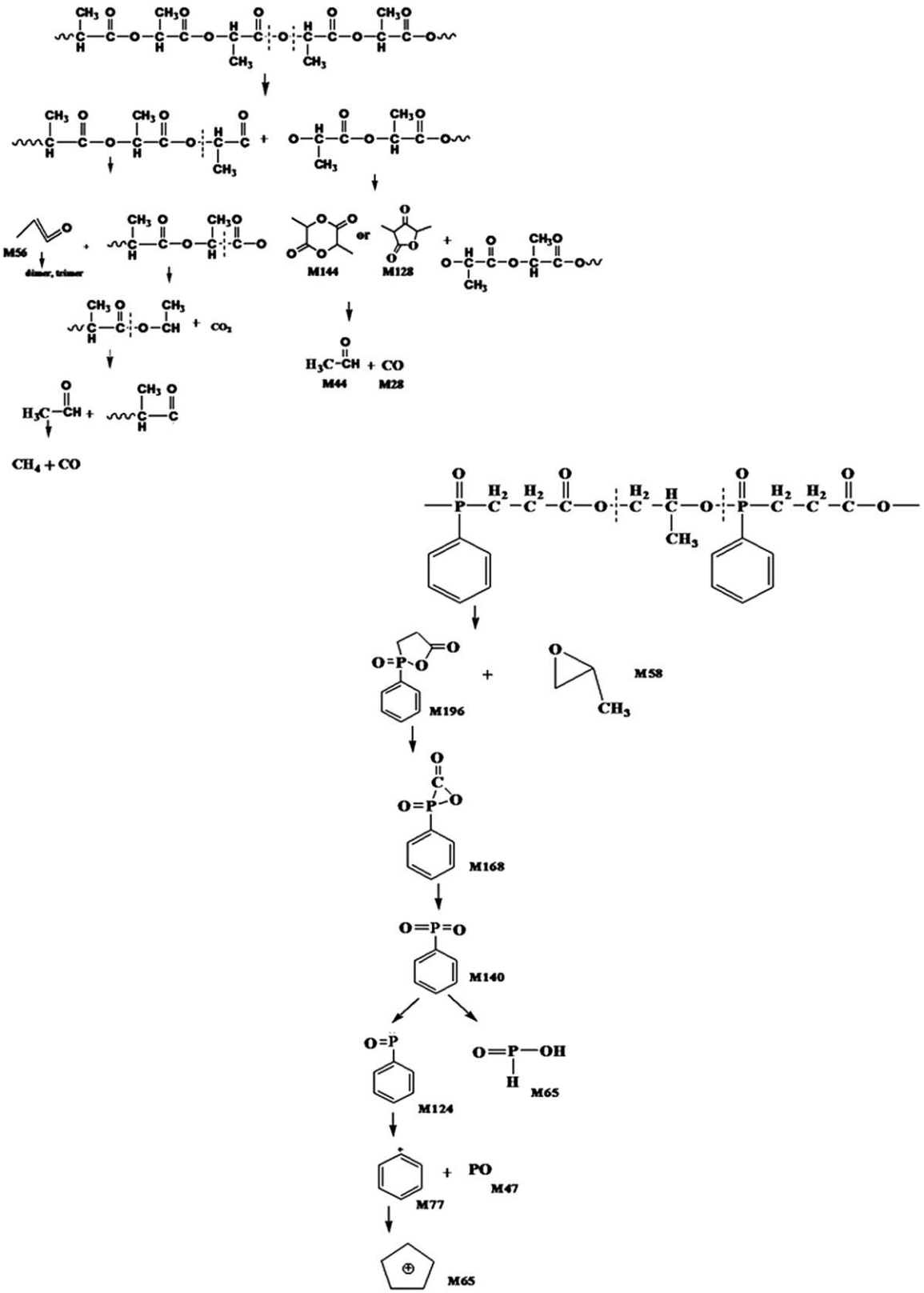

Figure 12. Oversimplified mass fragmentations of PLA and PCPP.

temperature of blend is raised to 450°C, only a small amount of pyrolysis products belonging to PLA is observed. That is PLA decomposes at the higher temperature in the PLA/15% PCPP blend. It means that PCPP decomposes mainly at the temperature of 350°C and the thermal stability of PLA blend improves with the addition of PCPP.

As Figure 11 shows, the mass spectrum at 350°C is mainly attributed to the decomposition of PCPP, such as 196 m/z for $C_9H_9PO_3$, 140 m/z for $C_7H_5PO_3$, and 47 m/z for PO ion. And other peaks at 140, 124, 77, and 65 m/z are from the degradation of phosphate. In the mass spectrum at 450°C, the peaks at 272, 128, 56, and 28 m/z can be assigned to the fragment ions that mainly results from the degradation of PLA. The oversimplified fragment of PLA and PCPP are shown in Figure 12 with the data from the mass fragmentations of the key TIC ions.

The PO ion is found in the Py–GC–MS analysis, so the gas-phase inhibition is inferred as a contributing factor to the overall flame-retardant effect for PLA/PCPP blend. The mechanism of gas-phase inhibition involves a destruction of hydrogen atoms which leads to an interruption of the combustion chain. Concerning the phosphorus-containing flame retardant, the mechanism of gas-phase inhibition can be deduced from the dependence of the quenching on the phosphorus concentration. The PO ion acts on the combustion chain as follows. For most polymer flames are limited by the branching step of the combustion chain, $H + O_2 \rightarrow OH + O$, which depends on the presence of hydrogen atoms. While, the phosphorus species act via a third-body mechanism, catalyzing the recombination of hydrogen atoms according to follow, $PO + H \rightarrow HPO$, $HPO + H \rightarrow H_2 + PO$. And the inhibition cannot involve a chemical scavenging of H atoms with consumption of phosphorus species. Therefore, the type of mechanism would not require a much higher inhibitor concentration in the flame to produce a retarding effect.[24] The ability of phosphorus to act as a flame quencher has been verified in the published studies: a comparison of the quenching efficiency of PCl_3 with phosphorus-free hydrogen compounds show that, on a molecular basis, phosphorus is about 12 times as effective as chlorine and more than twice as effective as bromine,[25] which might be the reason for the high flame-retardant performance of PCPP.

In addition, the phosphorous compounds released during the decomposition of PCPP may act by dilution because they are poorly combustible. In conclusion, the PCPP may act by flame inhibition or by dilution in the gas-phase to improve the flame-retardant property of PLA in the PLA/PCPP system.

CONCLUSION

Thermal degradation behaviors of PLA and PLA/15% PCPP blend were investigated. TGA analysis showed that the beginning degradation temperature of PLA/15% PCPP blend shifted to lower temperature due to the low degradation temperature of PCPP. The thermal degradation activation energy of the PLA/15% PCPP obtained via FWO method was about 10 kJ/mol lower than that of neat PLA when the conversion was lower than 10%. But the E_a of PLA/15% PCPP blend was higher than that of neat PLA at the same conversion when the conversion ranged from 10% to 80%. In a word, the beginning degradation temperature of the PLA/PCPP blend decreased in the presence of PCPP, but the thermal stability of PLA/PCPP was improved when the conversion was more than 10%. In addition, the appropriate conversion model of the process of the PLA/PCPP blend studied by Criado method was similar to that of the PLA at the main weight loss process. And TGA–FTIR was used to analyze the main gaseous decomposition products of PLA and its blend. It revealed that the unchanged compositions of the decomposition products were H_2O, CO_2, and hydrocarbons, etc. While the release of combustion pyrolysis products of PLA/15% PCPP blend was lower than that of neat PLA. Consequently, the PCPP flame retardant acted on the improvement of flame-retardant property of PLA by reducing the release of gaseous products (especially flammable gases) rather than changing the pyrolysis way. The flame retardant mechanism of gas-phase was further confirmed Py–GC–MS analysis. The PCPP acted by flame inhibition or by dilution to improve the flame-retardant property of PLA in the PLA/PCPP system.

ACKNOWLEDGMENTS

This study was supported by the National Science Foundation of China (51021003).

REFERENCES

1. Okada, M. *Prog. Polym. Sci.* **2002**, *27*, 87.
2. Lim, L. T.; Auras, R.; Rubino, M. *Prog. Polym. Sci.* **2008**, *33*, 820.
3. Liu, L. S.; Fishman, M. L.; Hicks, K. B.; Liu, C. *J. Agric. Food. Chem.* **2005**, *53*, 9017.
4. Auras, R.; Harte, B.; Selke, S. *Macromol. Biosci.* **2004**, *4*, 835.
5. Stevens, G. C.; Mann, A. H. Risks and Benefits in the Use Flame Retardants in Consumer Products; DTI Report: London, **1999**.
6. Granzow, A. *Acc. Chem. Res.* **1978**, *11*, 177.
7. Laoutid, F.; Bonnaud, L.; Alexandre, M.; Lopez-Cuesta, J. M.; Dubois, P. *Mater. Sci. Eng. R* **2009**, *63*, 100.
8. Sergei, V. L.; Edward, D. W. *Polym. Int.* **2005**, *54*, 11.
9. Lin, H. J.; Liu, S. R.; Han, L. J.; Wang, X. M.; Bian, Y. J.; Dong, L. S. *Polym. Degrad. Stab.* **2013**, *98*, 1389.
10. Flynn, J.; Wall, L. A. *Polym. Lett.* **1966**, *4*, 323.
11. Doyle, C. *J. Appl. Polym. Sci.* **1961**, *5*, 285.
12. Kissinger, H. *J. Res. Natl. Bur. Stand.* **1956**, *57*, 217.
13. Andricic, B.; Kovacic, T. *Polym. Degrad. Stab.* **1999**, *65*, 59.
14. Criado, J. M. *Thermochim. Acta* **1978**, *24*, 186.
15. Ignjatovic, N.; Suljovrujic, E.; Simendic, J. V.; Krakovsky, I.; Uskokovic, D. *J. Biomed. Mater. Res. B* **2004**, *71B*, 284.
16. Mohamed, A.; Gordon, S.; Biresaw, G. *J. Appl. Polym. Sci.* **2007**, *106*, 1689.
17. Braun, U.; Balabanovich, A. I.; Schartel, B. *Polymer* **2006**, *47*, 8495.
18. Wu, K.; Hu, Y.; Song, L.; Lu, H. D.; Wang, Z. Z. *Ind. Eng. Chem. Res.* **2009**, *48*, 3150.
19. Wu, K.; Song, L.; Hu, Y.; Lu, H. D.; Kandola, B. K.; Kandare, E. *Prog. Org. Coat.* **2009**, *65*, 490.

20. Wang, X.; Hu, Y.; Song, L.; Xuan, S. Y.; Xing, W.; Bai, Z. M.; Lu, H. *Ind. Eng. Chem. Res.* **2011**, *50*, 713.
21. Wang, X.; Hu, Y.; Song, L.; Xing, W. Y.; Lu, H. D.; Lv, P.; Jie, G. X. *Polymer* **2010**, *51*, 2435.
22. Fan, Y. J.; Nishida, H.; Mori, T.; Shirai, Y.; Endo, T. *Polymer* **2004**, *45*, 1197.
23. Fan, Y.; Nishida, H.; Hoshihara, S.; Shirai, Y.; Endo, T. *Polym. Degrad. Stab.* **2003**, *81*, 515.
24. Granaow, A. H. *Acc. Chem. Res.* **1978**, *11*, 177.
25. Lask, G.; Wagner, H. G. Eighth Symposium (International) on Combustion; Williams & Wilkins Co.: Baltimore, **1962**, p 432.